

Comparative Proteomics of Ovarian Cancer Aggregate Formation Reveals an Increased Expression of Calcium-activated Chloride Channel Regulator 1 (CLCA1)*[§]

Received for publication, January 20, 2015, and in revised form, May 21, 2015. Published, JBC Papers in Press, May 24, 2015, DOI 10.1074/jbc.M115.639773

Natasha Musrap^{‡§}, Alessandra Tuccitto^{‡§}, George S. Karagiannis^{‡§}, Punit Saraon^{‡§}, Ihor Batruch[§], and Eleftherios P. Diamandis^{‡§¶12}

From the [‡]Department of Laboratory Medicine and Pathobiology, University of Toronto, Toronto, Ontario, Canada M5S 1A8, the

[§]Department of Pathology and Laboratory Medicine, Mount Sinai Hospital, Toronto, Ontario, Canada M5T 3L9, and the

[¶]Department of Clinical Biochemistry, University Health Network, Toronto, Ontario, Canada M5G 2C4

Background: Cancer spheroid formation is a hallmark during ovarian cancer progression.

Results: Quantitative proteomics were used to delineate proteomic alterations during aggregate formation.

Conclusion: CLCA1 is elevated in ovarian cancer cell line aggregates.

Significance: CLCA1 and chloride channels may serve as novel therapeutic targets for ovarian cancer treatment.

Ovarian cancer is a lethal gynecological disease that is characterized by peritoneal metastasis and increased resistance to conventional chemotherapies. This increased resistance and the ability to spread is often attributed to the formation of multicellular aggregates or spheroids in the peritoneal cavity, which seed abdominal surfaces and organs. Given that the presence of metastatic implants is a predictor of poor survival, a better understanding of how spheroids form is critical to improving patient outcome, and may result in the identification of novel therapeutic targets. Thus, we attempted to gain insight into the proteomic changes that occur during anchorage-independent cancer cell aggregation. As such, an ovarian cancer cell line, OV-90, was cultured in adherent and non-adherent conditions using stable isotope labeling with amino acids in cell culture (SILAC). Anchorage-dependent cells (OV-90AD) were grown in tissue culture flasks, whereas anchorage-independent cells (OV-90AI) were grown in suspension using the hanging-drop method. Cellular proteins from both conditions were then identified using LC-MS/MS, which resulted in the quantification of 1533 proteins. Of these, 13 and 6 proteins were up-regulated and down-regulated, respectively, in aggregate-forming cells compared with cells grown as monolayers. Relative gene expression and protein expression of candidates were examined in other cell line models of aggregate formation (TOV-112D and ES-2), which revealed an increased expression of calcium-activated chloride channel regulator 1 (CLCA1). Moreover, inhibitor and siRNA transfection studies demonstrated an apparent effect of CLCA1 on cancer cell aggregation. Further elucidation of the role of CLCA1 in the pathogenesis of ovarian cancer is warranted.

For several years, ovarian cancer (OvCa)³ has been the most lethal gynecological malignancy among women in North America, where it accounts for 5% of all cancer-related deaths (1). Unfortunately, in most cases, the disease is not detected until advanced stages, at which point the cancer has progressed considerably. Despite recent efforts made toward the development of personalized treatment strategies for ovarian cancer, patient survival rates have barely improved since the arrival of platinum-based chemotherapy, with an overall average 5-year survival rate of 44% (1, 2). Meanwhile, the standard treatment for late stage patients continues to be cytoreductive surgery followed by chemotherapy (3). Although this approach may lead to a partial or complete remission, the probability that residual cancer cells not removed during surgery will develop resistance is high, and will eventually lead to recurrent disease (3). Beyond this point, the cancer is rendered incurable. Given that the majority of patients develop high-grade tumors, which are characterized by late stage presentation and intraperitoneal spread, there is an urgent need to understand OvCa metastasis and identify key molecules that drive tumor progression.

The formation of metastatic implants on the peritoneum relies on the detachment and spread of cancerous cells from the primary tumor (4). During this process, detached cells remain suspended in ascites fluid within the peritoneal cavity and form multicellular aggregates (MCAs), also known as spheroids, which obtain an anchorage-independent behavior that is resistant to apoptosis (4, 5). As such, recent emphasis has been placed on delineating the underlying biology of spheroid growth and formation given that these three-dimensional models are more representative of *in vivo* conditions, and share similar biological features to solid tumors (6). More importantly, it has been shown that MCAs facilitate ovarian cancer metastasis, by breaching the mesothelium and causing widespread peritoneal

* The authors declare that they have no conflicts of interest with the contents of this article.

[§] This article contains supplemental Table S1.

¹ Recipient of the Canadian Institutes of Health Research (CIHR) Doctoral Research Award.

² To whom correspondence should be addressed: Mount Sinai Hospital, Joseph and Wolf Lebovic Ctr., 60 Murray St., Box 32, 6th Floor, Rm. L6-201, Toronto, Ontario M5T 3L9, Canada. Tel.: 416-586-8443; Fax: 416-619-5521; E-mail: ediamandis@mtsinai.on.ca.

³ The abbreviations used are: OvCa, ovarian cancer; SILAC, stable isotope labeling with amino acids in cell culture; AD, anchorage-dependent; AI, anchorage-independent; CLCA1, calcium-activated chloride channel regulator 1; MCA, multicellular aggregate; NFA, niflumic acid; MUC5AC, mucin 5AC; CLIC, chloride intracellular channel protein.

dissemination (7–10). Numerous studies have highlighted the ability of spheroids to acquire chemoresistant, and stem-like properties, both of which have major implications for disease outcome (6, 11). Thus far, it is believed that interactions between various cell adhesion molecules and extracellular matrix components contribute to the formation of MCAs, including integrins, fibronectin, and cadherins (5, 7, 8, 12). Interestingly, studies have also shown that gene and protein expression can differ between cancer cells grown in monolayers *versus* those within multicellular aggregates (11, 13). Thus, a global comprehensive proteomics analysis that compares the proteome of the two cell populations may add to our current understanding about OvCa progression, as well as aid in the identification of novel therapeutic targets.

Over the past decade, advances in proteomic technologies have led to the quantitative identification of proteins in various biological samples using different labeling and non-labeling approaches (14). Such strategies offer several advantages, as they allow for a direct quantifiable comparison of proteins between samples to be performed, rather than being restricted to a qualitative analysis. In this study, a quantitative proteomics-based approach using stable isotope labeling of amino acids in cell culture (SILAC) (15) coupled to mass spectrometry (LC-MS/MS) was used to identify differentially expressed proteins in ovarian cancer cells (OV-90) cultured as aggregates (anchorage-independent, OV-90AI) compared with those cultured as monolayers (anchorage-dependent, OV90-AD). In total, 1533 proteins were quantified, as 13 and 6 proteins were overexpressed and underexpressed, respectively, in aggregate-forming cells compared with cells grown as monolayers. From our analysis, calcium-activated chloride channel regulator 1 (CLCA1) was significantly elevated during MCA formation, which was confirmed using other cell line models. By using chloride channel blockers, in addition to siRNA knockdown of CLCA1, we further demonstrated that CLCA1 has an effect on cell aggregation. Taken together, our findings reveal novel proteins that facilitate MCA formation, which may serve as potential therapeutic targets for the treatment of OvCa.

Experimental Procedures

Cell Lines—The human ovarian cancer cell lines, OV-90 (CRL-11732), TOV-112D (CRL-11731), and ES-2 (CRL-1978) were purchased from the American Type Culture Collection (ATCC, Manassas, VA). All cell lines were grown and maintained in RPMI 1640 medium (Gibco) supplemented with 10% characterized fetal bovine serum (FBS) (Thermo Scientific). All OvCa cells were maintained in a humidified incubator at 37 °C with an atmosphere of 5% CO₂.

Cell Culture/SILAC Labeling—OV-90 cells were seeded into T25 flasks and cultured using a modified version of RPMI 1640, which initially had lacked arginine and lysine amino acids (Athena ES, Baltimore, MD), but had been spiked with either “heavy” amino acids ([¹³C]_L-Arg⁶ and [¹³C,⁵N]_L-Lys⁸) (Cambridge Isotope Laboratories), or “light” amino acids ([¹²C]arginine and [¹²C,¹⁴N]lysine) (Sigma). The resulting SILAC media was then supplemented with 10% dialyzed FBS (Life Technologies) and additional L-proline amino acids were also added to reduce arginine isotope-conversion to proline in the cells (16).

Cells were then grown in heavy and light conditions for a period of five doubling times to ensure adequate labeling efficiency. During the last passage, light and heavy cells were each transferred to three T25 flasks and grown to confluence. Heavy labeled cells were used to generate cell line aggregates, using the hanging drop method (17–18), whereas light labeled cells were maintained in adherent conditions. Briefly, heavy labeled cells were suspended from the top of a Petri dish plate that contained 10–15 ml of PBS. Each condition was conducted in three experimental replicates. After a period of 2 days, cell pellets from each replicate was collected, washed twice with PBS, and stored at –80 °C. Monolayers and multicellular aggregates of OV-90, TOV-112, and ES-2 cells used in mRNA and Western blot analyses were generated in the same method as described above, with the exception that regular RPMI supplemented with 10% FBS was used.

Sample Preparation and Strong Cation Exchange of SILAC-labeled Cells for Mass Spectrometry—Cell pellets were resuspended and lysed in 250 μl of 0.1% RapiGest (Waters Inc., Milford, MA) in 25 mM ammonium bicarbonate, vortexed, and then sonicated for 30 s. The resulting lysates were then centrifuged at 4 °C for 15 min at 10,000 × g to remove cellular debris. The total protein concentration of each sample was measured using a Coomassie (Bradford) protein assay and cell lysates from heavy and light labeled cells were combined in a 1:1 total protein ratio. The samples were then denatured at 80 °C for 15 min, reduced with 10 mM dithiothreitol, and alkylated with 20 mM iodoacetamide for 1 h. Proteins were digested overnight at 37 °C with trypsin using a trypsin:total protein ratio of 1:50 (Sigma). Samples were acidified with 1% trifluoroacetic acid to cleave RapiGest, which was then removed by centrifugation.

Samples containing tryptic peptides were diluted with mobile phase buffer A (0.26 M formic acid, 10% acetonitrile) to a final volume of 500 μl. The entire sample was then loaded onto a PolySULFOETHYL A column containing an anionic polymer with pore sizes of 0.02 μm and a diameter of 5 μm (The Nest Group Inc., MA). The column was connected to an Agilent 1100 high performance liquid chromatography system. Peptides were fractionated and eluted using a 1-h gradient of a buffer that consisted of mobile phase A with the addition of 1 M ammonium formate. The separation was monitored at a wavelength of 280 nm and fractions were collected every 2 min from 24 to 50 min with a flow rate of 200 μl/min. The last two fractions, which displayed the lowest peak absorbance, were pooled, resulting in a total of 12 fractions per replicate. Fractions were then diluted to achieve a final acetonitrile concentration of 5%.

Mass Spectrometry—Peptides from each fraction were purified and extracted using OMIX C₁₈ Pipette Tips, and eluted in 70% MS Buffer B (90% acetonitrile, 0.1% formic acid, 10% water, and 0.02% trifluoroacetic acid) and 30% MS Buffer A (5% acetonitrile, 0.1% formic acid, 95% water, and 0.02% trifluoroacetic acid). Approximately 40 μl of each fraction was loaded onto an EASY-nLC system (Proxeon Biosystems, Denmark), which was coupled online to an LTQ-Orbitrap mass spectrometer (Thermo Fisher Scientific). Peptides were first loaded onto a 3-cm C₁₈ trap column, and eluted peptides were then resolved using a 5-cm analytical C₁₈ column with a 90-min gradient of

Proteomic Delineation of Ovarian Cancer Cell Line Aggregates

MS buffers and A and B, using data-dependent mode. Peptides were subjected to one full MS1 scan (450–1450 m/z) in the Orbitrap (60,000 resolution), and six MS2 scans in the linear ion trap mass analyzer. Using charge state screening, only ions with charge states of +2 and +3 were selected to undergo MS2 fragmentation.

Data Analysis and Protein Quantitation—RAW files generated with XCalibur software (version 2.05, Thermo Fisher Scientific) that contained mass spectra of all identified peptides were analyzed using MaxQuant software (version 1.2.2.5) and searched against the International Protein Index human database (version 3.71). The maximum number of modifications per peptide was set to 5, along with a maximum of two missed cleavages. Both a peptide and protein false discovery rate of 1% were selected, and a minimum of 2 unique peptides were chosen for protein identification. Re-quantification and match between runs were specified. The resulting median normalized heavy/light ratios of experimental replicates were used for further study and selection of candidates.

Using the data output produced by MaxQuant software, the standard deviation (95% confidence interval) of Log_2 -transformed ratios was computed. The z -score and p values were calculated based on the assumption that the log ratios were zero. The resulting p values were then corrected for multiple testing using the Benjamini-Hochberg method (19), which was used to control the false discovery rate. Proteins with adjusted p values (q values) less than 0.05 were chosen as possible candidates.

International Protein Index numbers of overexpressed and underexpressed candidates were loaded into ProteinCenter, and categorized according to their molecular and biological functions using predicted gene ontology annotations. Top cellular and molecular functions of candidate proteins were determined using Ingenuity Pathway Analysis software (Ingenuity® Systems).

mRNA Expression Analysis—Total RNA was extracted from cell pellets using an RNeasy Kit (Qiagen). A SuperScript First-strand cDNA synthesis kit (Invitrogen) was used to synthesize complementary DNA for subsequent quantitative PCR. *GAPDH* (glyceraldehyde-3-phosphate-dehydrogenase) was used as an endogenous control to normalize the relative expression of the top six SILAC candidate genes: *SLC1A5*, *SERPIND1*, *MAOB*, *CLCA1*, *FNI*, and *CES1*. Forward and reverse primer sequences were: *GAPDH*, TCTCCTCTGACTCAACAGCG (forward) and ACCACCCTGTTGCTGTAGCCAA (reverse); *SLC1A5*, TCCTCTTACCCGCAAAAACCC (forward) and CCACGCATTATTCTCCTCCAC (reverse); *SERPIND1*, GTGGAGTCCCTGAAGTTGATGG (forward) and CCTTCTCGTTCATCTGTGATCG (reverse); *MAOB*, GTGAAGCAGTGTGGAGGCACAA (forward) and TTCCTATGACAACACAGCC (forward) and GTCGATTGAGGCGGTTACCAGT (reverse); *FNI*, ACAACACCGAGGTGACTGAGAC (forward) and GGACACAACGATGCTTCC-TGAG (reverse); *CES1*, ATCCACTCTCCGAAGGGCAACT (forward) and GACAGTGTCTGTTCCTCCT (reverse). Quantitative PCR were performed using SYBR Green PCR Master Mix (Applied Biosystems), and carried out on a 7500

ABI system. Relative gene expression was calculated using the comparative C_t method (20).

Western Blot—Cell pellets (OV-90 and OV-90S; TOV-112D and TOV-112DS; ES-2 and ES-2S) were lysed with 1× Cell Lysis Buffer (Cell Signaling Technology) containing 1 mM PMSF (phenylmethanesulfonyl fluoride) and sonicated for 30 s. The samples were then centrifuged at $15,000 \times g$ for 10 min to remove any cellular debris. The total protein concentration was determined using the Bradford protein assay and equal amounts of total protein from each sample were loaded onto an SDS-PAGE gel (Bio-Rad). After electrophoresis, proteins were transferred onto polyvinylidene fluoride (PVDF) membranes (Bio-Rad) and blocked overnight at 4 °C. A primary rabbit polyclonal antibody against CLCA1 (Santa Cruz) was used to examine protein expression in cell lysates.

Treatment with Chloride Channel Blocker, Niflumic Acid (NFA)—Niflumic acid (Sigma) was prepared in dimethyl sulfoxide as a $\times 1000$ stock solution, which allowed for the final concentration of dimethyl sulfoxide used in experimental stimulations to be low. Cells were grown in six-well plates and pretreated with 100 μM NFA for a period of 5 h before generating MCAs, whereas control cells were maintained in regular growth medium. After 5 h, treated and control cells were grown in anchorage-independent conditions for a period of 48 h in either regular medium or medium containing 100 μM NFA before the aggregates were collected and imaged.

Cell Viability Assay—To determine whether niflumic acid had an effect on cell viability, an alamarBlue assay (Invitrogen) was performed. Briefly, cells (OV-90, TOV-112D, and ES-2) were seeded into 96-well plates for 24 h, and different concentrations of NFA were used to treat the cells, which was performed in triplicates. After 24 h, 1/10th volume of alamarBlue reagent was added to cell culture medium, and the culture was incubated at 37 °C for 2 h. The reagent was detected by measuring absorbance at 570 nm using a plate reader, and differences in cell viability were assessed.

Cell Adhesion Assay—96-Well plates were coated with 10 $\mu\text{g}/\text{ml}$ of fibronectin overnight at 4 °C. Afterward, the plates were incubated with 0.2% BSA for 1 h at 37 °C to block nonspecific binding sites. Approximately 4×10^5 cells were plated in each well with RPMI medium that either contained or did not contain 100 $\mu\text{mol}/\text{liter}$ of NFA and were allowed to attach for 1.5 h. Unattached cells were removed from the wells by aspiration, and the relative abundance of the adhered cells was assessed using alamarBlue. Changes in optical density were analyzed by measuring absorbance at 540 nm. All experiments were performed in technical triplicates.

siRNA Transfections for CLCA1—siGENOME SMARTpool siRNAs for CLCA1 (Dharmacon) and non-targeting siRNA pools were purchased from GE Healthcare and transfections were performed according to the recommended protocol. Briefly, cells (OV-90, TOV-112D, and ES-2) were seeded in six-well plates and transfected with target and non-target oligonucleotides using DharmaFECT1 Transfection Reagent with a final siRNA concentration of 50 nM. After 3 days, the cells were collected and the ability to form aggregates was examined by culturing cells in MCAs as described above. Transfected cells

Proteomic Delineation of Ovarian Cancer Cell Line Aggregates

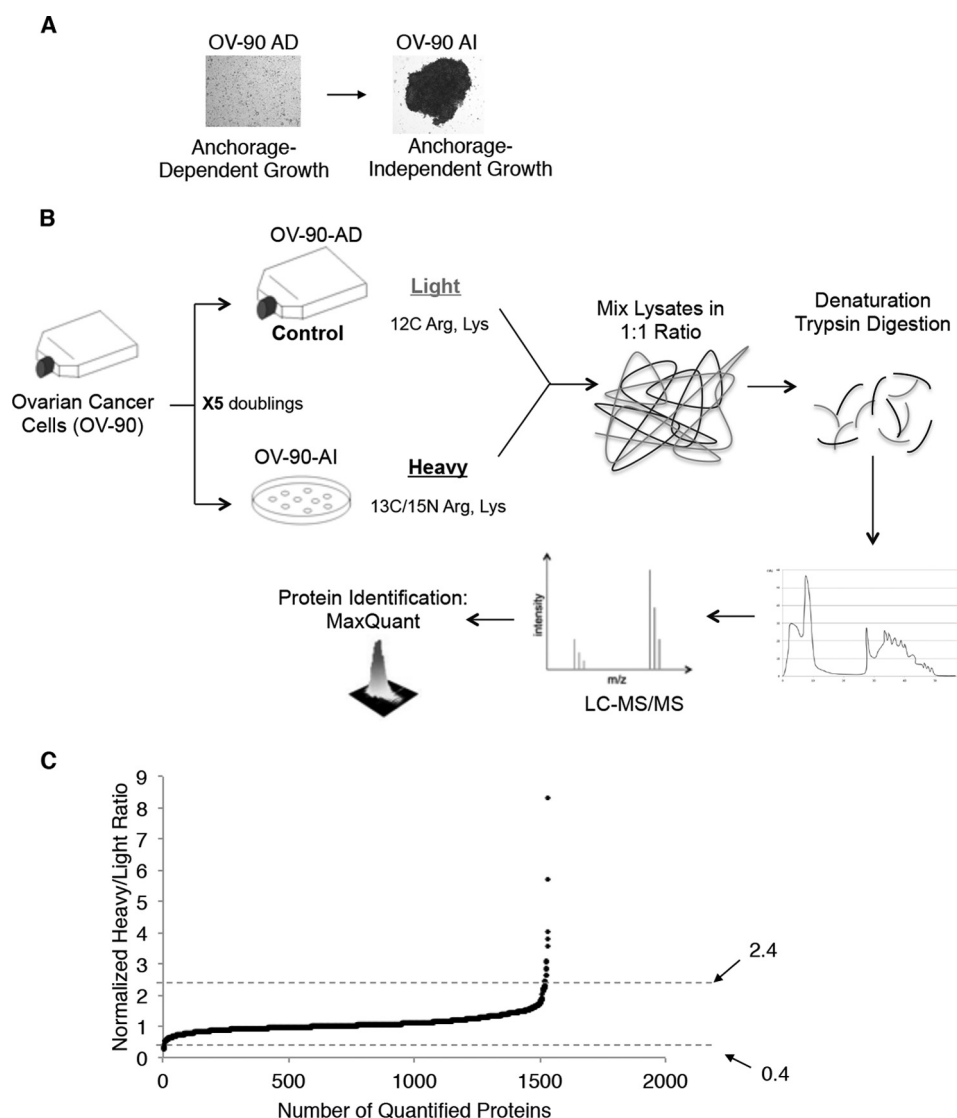


FIGURE 1. *A*, OV-90 cells were grown in anchorage-dependent and -independent conditions using the hanging drop method. Images are displayed at $\times 40$ magnification. *B*, schematic representation of the SILAC-based proteomic workflow used to identify differentially expressed proteins. *C*, graphical plot illustrating the number of quantified proteins with various heavy/light ratios. Proteins that displayed ratios above 2.4 and below 0.4 were considered statistically significant. More details or experimental procedures can be found in the text.

were also collected to assess the protein expression of CLCA1 using Western blot analysis.

Statistical Analysis—All statistical significance tests on gene expression, Western blot, cell viability, and cell adhesion data were analyzed using independent *t*-tests (Minitab, version 14). Results were considered significant if the *p* value was less than or equal to 0.05.

Results

MS Identification of Proteins Differentially Expressed during MCA Formation—To identify proteins that displayed differential expression during ovarian cancer cell line aggregate formation, we conducted a comparative proteomics analysis, in which we quantitatively compared the expression of proteins identified in lysates of cells grown as monolayers to those grown as aggregates. As such, SILAC was used to label proteins in each condition by growing cells (OV-90) in media containing heavy and light arginine and lysine isotopes (Fig. 1, *A* and *B*). For each

protein identified, a heavy/light (H/L) ratio was generated using MaxQuant software, which represents the abundance of a particular protein in each condition. Overall, our analysis resulted in the quantification of 1533 proteins with a minimum of two peptides. To identify candidates that were differentially regulated between the two conditions, we chose proteins whose *q* values were less than 0.05, which represent *p* values corrected for multiple testing (Benjamini-Hochberg, false discovery rate of 5%). As a result, with this definition, 13 and 6 proteins were overexpressed and underexpressed, respectively, in aggregate-forming cells compared with cells grown as monolayers, using cut-off ratios of 2.4 and 0.4 (Fig. 1C and Tables 1 and 2). Proteins that displayed ratios between 0.4 and 2.4 were not considered to show a significant change in protein expression. To confirm the accuracy of our ratios, we examined H/L ratios of housekeeping proteins, which are expected to display the same level of protein expression in both conditions. Overall, various control proteins displayed H/L ratios close to 1, including

TABLE 1
Normalized median H/L ratios of overexpressed SILAC candidates

Accession	Gene symbol	Protein description	Normalized H/L ratio	<i>q</i> value ^a
IPI00014625	<i>CLCA1</i>	Calcium-activated chloride channel regulator 1	8.30	3.91E-14
IPI00607801	<i>CES1</i>	Isoform 2 of liver carboxylesterase 1	5.72	2.26E-09
IPI00939667	<i>TPP1</i>	Tripeptidyl-peptidase 1 preproprotein	4.03	9.26E-06
IPI00877703	<i>FGG</i>	Uncharacterized protein	3.81	2.63E-05
IPI00845263	<i>FN1</i>	Fibronectin isoform 4 preproprotein	3.56	8.69E-05
IPI00328156	<i>MAOB</i>	Amine oxidase (flavin-containing) B	3.08	1.15E-03
IPI00413451	<i>SERPINB6</i>	Serpin B6	3.05	1.27E-03
IPI00007709	<i>ADAM28</i>	Isoform 1 of disintegrin and metalloproteinase domain-containing protein 28	2.87	3.07E-04
IPI00292950	<i>SERPIND1</i>	Serpin peptidase inhibitor, clade D	2.82	4.07E-03
IPI00019872	<i>HSD17B2</i>	Estradiol 17- β -dehydrogenase 2	2.65	1.08E-02
IPI00023001	<i>FAM162A</i>	Protein FAM162A	2.62	1.09E-02
IPI00289159	<i>GLS</i>	Isoform 1 of glutaminase kidney isoform, mitochondrial	2.45	2.81E-02
IPI00005668	<i>AKR1C2</i>	Aldo-keto reductase family 1 member C2	2.43	3.05E-02

^a*q* value: adjusted *p* value corrected for multiple testing (Benjamini-Hochberg method).

TABLE 2
Normalized median H/L ratios of underexpressed SILAC candidates

Accession	Gene symbol	Protein description	Normalized H/L ratio	<i>q</i> value ^a
IPI00554777	<i>ASNS</i>	Asparagine synthetase (glutamine-hydrolyzing)	0.24	8.07E-06
IPI00217950	<i>HMGN2</i>	Non-histone chromosomal protein HMG-17	0.31	7.84E-04
IPI00028270	<i>CEACAM7</i>	Isoform 2a of carcinoembryonic antigen-related cell adhesion molecule 7	0.32	1.14E-03
IPI00008475	<i>HMGCS1</i>	Hydroxymethylglutaryl-CoA synthase, cytoplasmic	0.33	1.45E-03
IPI00019472	<i>SLCIA5</i>	Neutral amino acid transporterB (0)	0.38	1.09E-02
IPI00027486	<i>CEACAM5</i>	Carcinoembryonic antigen-related cell adhesion molecule 5	0.41	2.81E-02

^a*q* value: adjusted *p* value corrected for multiple testing (Benjamini-Hochberg method).

GAPDH (0.98), RPL27A (0.98), and RPS20 (0.91). Mass spectra of peptides for promising candidates were further examined and six proteins (SLCIA5, SERPIND1, MAOB, CLCA1, FN1, and CES1) were chosen for further study (Fig. 2).

Gene Ontology annotations available through Protein Center software were used to classify candidate proteins based on their biological processes and molecular functions, which included metabolic processes and nucleotide and protein binding, respectively. Ingenuity Pathway Analysis software (Ingenuity® Systems) was also used to reveal top molecular and cellular functions related to our candidates, which included small molecule biochemistry, lipid metabolism, molecular transport, and cell death and survival (Table 3).

Gene Expression Validation of Top Candidates Using In Vitro Models of Aggregate Formation—Quantitative PCR was used to examine the mRNA expression of top SILAC candidates in three ovarian cancer cell line models of MCA formation, including OV-90, TOV-112D, and ES-2. Each cell line was grown in anchorage-dependent and -independent conditions as described above, and relative expression of the above genes was compared in cells grown as MCAs and monolayers (data not shown). Of the genes examined, both *CLCA1* (Fig. 3A) and *CES1* (data not shown) showed significant increases in mRNA expression when OV-90 and ES-2 cells were grown as MCAs ($p < 0.05$, independent *t* test), which indicates that they may play an important role in OvCa progression.

Validation of CLCA1 Protein Expression in Cell Line Models of Aggregate Formation—The top candidate identified in our proteomic discovery, *CLCA1*, displayed a 8-fold increase in OV-90 cells that were grown in anchorage-independent conditions. To confirm the increase in protein expression of *CLCA1* during the formation of multicellular aggregates, Western blotting was performed on three cell lines that were grown as monolayers and as aggregates (OV-90/OV-90S, TOV-112D/

TOV-112DS, and ES-2/ES-2S). Overall, there was a significant increase in expression of *CLCA1* during aggregate formation in two cell lines, OV-90 and ES-2 ($p < 0.05$, independent *t* test), with no difference observed in TOV-112D cancer cells (Fig. 3B).

CLCA1 Blocker Affects Cell Adhesion and Multicellular Aggregation—The effect that *CLCA1* has on cancer cell adhesion to components of the extracellular matrix was examined using the *CLCA1* inhibitor, NFA. NFA is a blocker of calcium-activated chloride channels and inhibits *CLCA1* function (21–22). Briefly, cancer cells were added to fibronectin-coated plates in the absence or presence of NFA. Overall, cell adhesion of OV-90 and ES-2 cells was slightly reduced after 1.5 h when cells were treated with NFA compared with the control condition as illustrated in Fig. 4B ($p < 0.05$).

To assess the role of *CLCA1* in aggregate formation, cancer cells were treated with NFA. Briefly, OV-90, TOV-112D, and ES-2 cells were pre-treated with 100 μ M NFA for a period of 5 h along with untreated cells, before creating OvCa cell line aggregates. After a period of 48 h, it was shown that blocking chloride channels resulted in a reduced ability for cancer cells to form aggregates (Fig. 4C). To confirm that the observed effects on cell aggregation were due to the blocking ability of NFA and not due to decreased cell viability, an alamarBlue assay was performed. Cells were treated with the same concentration of NFA used in the above experiment for a period of 24 h, which resulted in no significant change in cell viability (Fig. 4A).

siRNA Knockdown and MCA Formation with CLCA1 siRNA-transfected Cells—The protein expression of *CLCA1* was assessed in siRNA-transfected OV-90, TOV-112D, and ES-2 cells using Western blot analysis. Seventy-two hours after *CLCA1* siRNA transfection, the protein expression of *CLCA1* had decreased, compared with cells transfected with non-targeting siRNAs (Fig. 5A). To examine the effect of *CLCA1* on cell

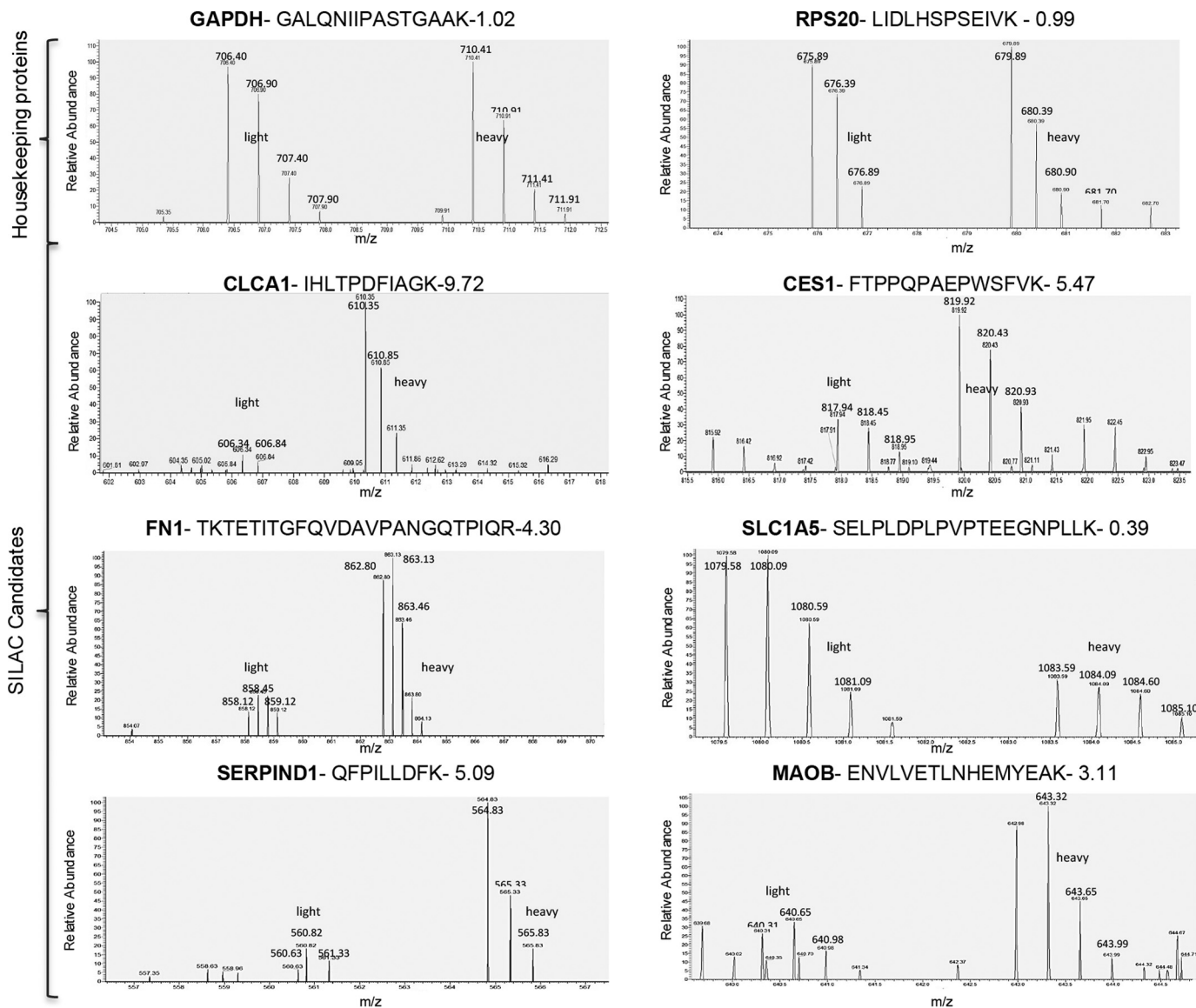


FIGURE 2. Heavy and light spectra of representative peptides from housekeeping proteins (GAPDH and RPS20) and candidate proteins (CLCA1, CES1, FN1, SLC1A5, SERPIND1, and MAOB) that were further validated in other cell line models.

TABLE 3

Molecular and cellular functions of proteins that are up-regulated and down-regulated during MCA formation

Name	<i>p</i> value	No. of proteins
Molecular and cellular functions of overexpressed proteins		
Lipid metabolism	2.52E-11 – 1.86E	18
Molecular transport	2.52E-11 – 1.86E-02	12
Small molecule	2.52E-11 – 1.86E	21
Biochemistry		
Energy production	1.31E-05 – 1.40E-02	4
Carbohydrate metabolism	3.18E-05 – 1.16E-02	6
Molecular and cellular functions of underexpressed proteins		
Lipid metabolism	2.19E-04 – 3.20E-02	5
Small molecule biochemistry	2.19E-04 – 4.92E-02	14
Vitamin and mineral metabolism	2.19E-04 – 2.09E-02	4
Cell death and survival	4.33E-04 – 4.77E-02	10
Gene expression	1.00E-03 – 3.25E-03	2

aggregation, CLCA1 siRNA-transfected and control cells were used to form aggregates as described above. After a period of 24 h, the ability to form compact aggregates was reduced (Fig. 5B).

Discussion

The formation of multicellular aggregates in ascites fluid of ovarian cancer patients plays a major role in ovarian cancer metastasis and has important implications for cancer therapy.

Proteomic Delineation of Ovarian Cancer Cell Line Aggregates

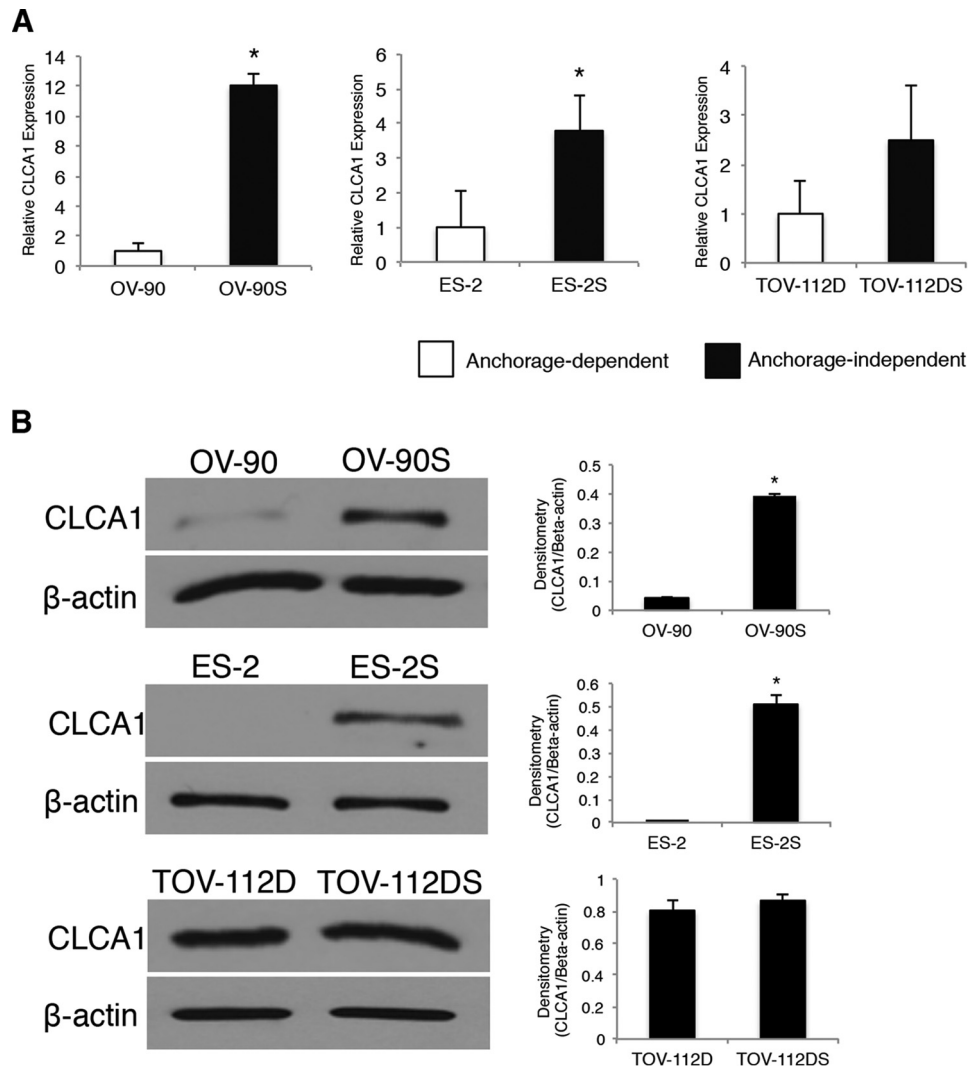


FIGURE 3. *A*, relative *CLCA1* mRNA expression in cell lines cultured as monolayers and MCAs. *B*, Western blot validation of *CLCA1* in cells grown in anchorage-dependent and -independent conditions (*, $p \leq 0.05$, independent *t* test; error bars represent S.D.).

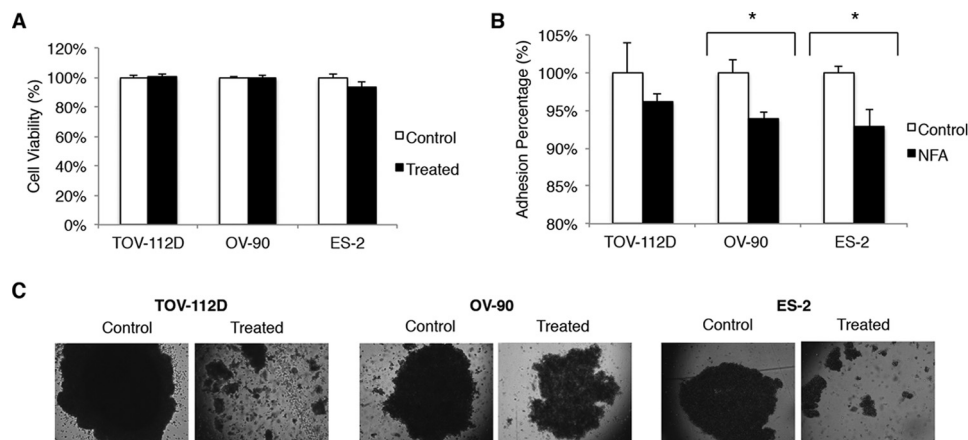


FIGURE 4. **Treatment of cancer cell lines with NFA.** *A*, cells did not display a significant change in cell viability when treated with $100 \mu\text{M}$ NFA for 24 h. *B*, OV-90 and ES-2 cell displayed a reduction in cell adhesion to fibronectin in the presence of $100 \mu\text{M}$ NFA after 1.5 h (*, $p \leq 0.05$, independent *t* test; error bars represent S.D.). *C*, cells displayed decreased cell aggregation when treated with NFA (48 h). All images are displayed at $\times 40$ magnification.

Recent studies have highlighted that cell behavior and gene expression profiles vary between cells grown in monolayers *versus* those that are grown as MCAs (11, 23). Given that these differences result in an increased invasiveness and chemoresis-

tance, a better understanding of how these spheroids form could lead to more effective approaches to treat the disease. As such, unraveling proteomic alterations during the transformation of cancer cells into a more dominant and malignant phe-

Proteomic Delineation of Ovarian Cancer Cell Line Aggregates

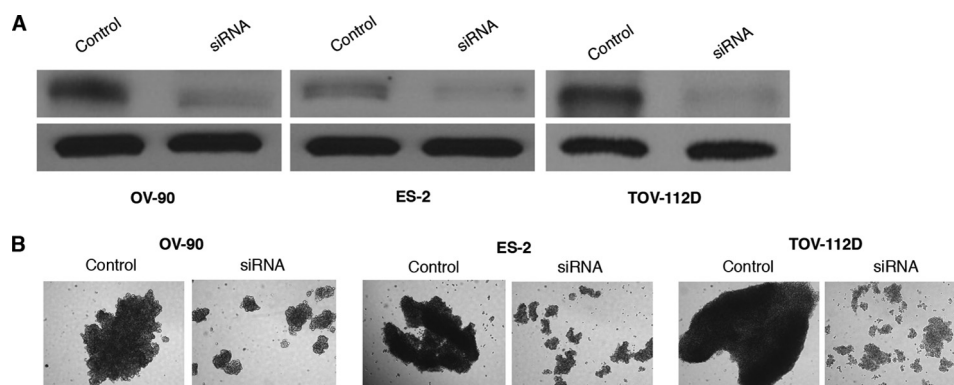


FIGURE 5. *A*, Western blot of control and CLCA1 siRNA-transfected OV-90, TOV-112D, and ES-2 cells. *B*, multicellular aggregates generated with transfected cells. All images are displayed at $\times 40$ magnification.

notype may result in the identification of novel therapeutic targets that may improve patient survival.

In this study, we undertook a comparative mass spectrometry-based approach to identify changes in proteomic expression during anchorage-independent and -dependent growth of the ovarian cancer cell line, OV-90. This cell line was chosen as our model system because its ability to form MCAs has been well established (24). Overall, our analysis resulted in the identification of 1533 proteins, of which 13 were overexpressed and 6 were underexpressed in MCA-forming cells. The majority of proteins identified did not display differential expression as they fell between our chosen cut-off ratios. Interestingly, one of the top SILAC candidates, fibronectin 1 (FN1), has been previously described as a promoter of spheroid formation through its interaction with $\beta 1$ -integrin, which further strengthens our findings (25).

We do acknowledge some limitations of our study. For instance, we included one cell line for our proteomic discovery, which may result in cell line biases. Given the complexity of OvCa, it would be expected that proteomes would differ among various cell lines. To account for this drawback, we evaluated our top candidates in other cell line models. Furthermore, although MCAs are believed to reflect solid tumors, our *in vitro* model lacks the contribution of the surrounding tumor microenvironment, including external signals that would be present in ascites fluid.

To confirm our preliminary data, we analyzed the mRNA expression of our top candidate proteins in three cell line models (OV-90, TOV-112D, and ES-2), which revealed a significant elevation of CLCA1 in two of the three cell lines (OV-90 and ES-2) when cultured as multicellular aggregates. Furthermore, protein expression validation using Western blot analysis corresponded with our gene expression data, as CLCA1 also displayed increased protein expression in OV-90 and ES-2 MCAs, with little or no difference observed in TOV-112D cell line aggregates. These differences observed between cell lines may be due to disease heterogeneity, or could be attributed to the fact that the cell lines are representative of different ovarian cancer subtypes.

To determine whether CLCA1 has a role in cell aggregation, experiments that blocked its activity or reduced its expression were performed. In both cases, treating cells with a chloride channel blocker, NFA, or using siRNAs to knockdown CLCA1

resulted in a reduced ability of cells to form aggregates. Interestingly, decreased aggregation for siRNA experiments was observed after a period of only 24 h, as reduced cell aggregation was not observed after 48 h. This finding indicates that other proteins are also involved in OvCa cell line aggregate formation. Moreover, even though TOV-112D did not display differences in CLCA1 expression during anchorage-dependent or -independent growth, the inhibitor was also able to reduce cell aggregation of this cell line. This suggests that the activity or function of CLCA1 is important for anchorage-independent growth and adhesion, and may help cells resist anoikis.

Given that multicellular aggregates are formed within ovarian cancer ascites fluid, it is reasonable to expect that proteins identified in our analysis, particularly those that are extracellular or membrane bound, would be detected in these proximal fluids as well. As such, a couple of our top candidates were also discovered in previous proteomic analyses of ovarian cancer ascites fluid (26–29), including FN1 and SERPIND1. Although, CLCA1 was not found in these fluids, several chloride channel-related proteins, such as chloride intracellular channel protein (CLIC) 1, CLIC4, and CLIC5, were detected (27–29). These observations suggest that these proteins may have important roles in cancer progression.

CLCA1 is a transmembrane protein that belongs to a family of ion channels that regulate calcium-dependent chloride conductance, and has been implicated in numerous biological processes (30, 31). These include epithelial secretion, cell-cell adhesion, mucus production, and apoptosis (31). Various chloride channels have been implicated in playing a role in ovarian cancer tumorigenesis, by promoting tumor-stroma interactions, and facilitating cancer metastasis (32). For instance, in a recent study, it was shown that chloride channels blockers, including NFA, were able to decrease proliferation, adhesion, and invasion of an ovarian cancer cell line, A2780 (33). Therefore, we also examined the effect of CLCA1 on the adhesion ability of our cancer cell lines to fibronectin, in which the adhesion rate was slightly reduced by 5% after 1.5 h. Such findings support our results, and indicate that CLCA1 plays a major role in cancer metastasis. In addition to OvCa, aberrant expression has also been reported in colorectal cancer, as CLCA1 was shown to regulate the proliferation and differentiation of a colon cancer cell line (34).

CLCA1 has also been implicated in other diseases, as studies have documented an increased level in inflammatory airway conditions, such as asthma, where it plays a role in mucus production (35). In particular, *CLCA1* has been associated with the hypersecretion of mucin 5AC (*MUC5AC*), as both genes are induced in upper airway mucosal explant tissue upon stimulation with TNF- α (21, 22, 36). In these studies, treatment of bronchial epithelial cells with the chloride channel blocker, NFA, resulted in decreased *MUC5AC* mRNA expression; however, the mechanism by which *CLCA1* regulates *MUC5AC* has yet to be elucidated (21, 36). We have previously reported an increased expression of *MUC5AC* during ovarian cancer-peritoneal interaction (37). Whether *CLCA1* controls the expression of *MUC5AC* in ovarian cancer requires further investigation.

In summary, we have conducted a comparative proteomics analysis, which revealed several proteins that display differential expression during cancer metastasis. Our findings provide new insight into the mechanisms of MCA formation, as we have identified proteins that may contribute to ovarian cancer pathogenesis. Further investigation into the role of *CLCA1* in ovarian cancer biology is needed, as future efforts should gear toward understanding the effects of *CLCA1* on cell survival and cancer resistance to chemotherapeutic drugs, in addition to assessing its role in cell aggregation *in vivo*.

Author Contributions—N. M. designed, performed, and analyzed the experiments and wrote the paper. A. T., G. S. K., and P. S. helped perform and analyze the experiments in Figs. 3–5. I. B. assisted with mass spectrometry experiments. E. P. D. contributed to the conception and design of the study, and helped draft and revise the manuscript. All authors reviewed the results and approved the final version of the manuscript.

Acknowledgments—We thank Apostolos Dimitromanolakis for analyzing SILAC data and Jane Bayani for insightful discussions.

References

1. Siegel, R., Ma, J., Zou, Z., and Jemal, A. (2014) Cancer statistics, 2014. *CA Cancer J. Clin.* **64**, 9–29
2. Vaughan, S., Coward, J. I., Bast, R. C., Jr., Berchuck, A., Berek, J. S., Brenton, J. D., Coukos, G., Crum, C. C., Drapkin, R., Etemadmoghadam, D., Friedlander, M., Gabra, H., Kaye, S. B., Lord, C. J., Lengyel, E., Levine, D. A., McNeish, I. A., Menon, U., Mills, G. B., Nephew, K. P., Oza, A. M., Sood, A. K., Stronach, E. A., Walczak, H., Bowtell, D. D., and Balkwill, F. R. (2011) Rethinking ovarian cancer: recommendations for improving outcomes. *Nat. Rev. Cancer* **11**, 719–725
3. Pignata, S., Cannella, L., Leopardo, D., Pisano, C., Bruni, G. S., and Facchini, G. (2011) Chemotherapy in epithelial ovarian cancer. *Cancer Lett.* **303**, 73–83
4. Shield, K., Ackland, M. L., Ahmed, N., and Rice, G. E. (2009) Multicellular spheroids in ovarian cancer metastases: biology and pathology. *Gynecol. Oncol.* **113**, 143–148
5. Casey, R. C., Bursleson, K. M., Skubitz, K. M., Pambuccian, S. E., Oegema, T. R., Jr., Ruff, L. E., and Skubitz, A. P. (2001) β 1-Integrins regulate the formation and adhesion of ovarian carcinoma multicellular spheroids. *Am. J. Pathol.* **159**, 2071–2080
6. Lee, J. M., Mhawech-Fauceglia, P., Lee, N., Parsanian, L. C., Lin, Y. G., Gayther, S. A., and Lawrenson, K. (2013) A three-dimensional microenvironment alters protein expression and chemosensitivity of epithelial ovarian cancer cells *in vitro*. *Lab. Invest.* **93**, 528–542
7. Iwanicki, M. P., Davidowitz, R. A., Ng, M. R., Besser, A., Muranen, T.,

- Merritt, M., Danuser, G., Ince, T. A., and Brugge, J. S. (2011) Ovarian cancer spheroids use myosin-generated force to clear the mesothelium. *Cancer Discov.* **1**, 144–157
8. Shield, K., Riley, C., Quinn, M. A., Rice, G. E., Ackland, M. L., and Ahmed, N. (2007) α 2 β 1 Integrin affects metastatic potential of ovarian carcinoma spheroids by supporting disaggregation and proteolysis. *J. Carcinog.* **6**, 11
9. Bursleson, K. M., Casey, R. C., Skubitz, K. M., Pambuccian, S. E., Oegema, T. R., Jr., and Skubitz, A. P. (2004) Ovarian carcinoma ascites spheroids adhere to extracellular matrix components and mesothelial cell monolayers. *Gynecol. Oncol.* **93**, 170–181
10. Bursleson, K. M., Hansen, L. K., and Skubitz, A. P. (2004) Ovarian carcinoma spheroids disaggregate on type I collagen and invade live human mesothelial cell monolayers. *Clin. Exp. Metastasis* **21**, 685–697
11. Condello, S., Morgan, C. A., Nagdas, S., Cao, L., Turek, J., Hurley, T. D., and Matei, D. (2015) β -Catenin-regulated ALDH1A1 is a target in ovarian cancer spheroids. *Oncogene* **34**, 2297–2308
12. Usui, A., Ko, S. Y., Barengo, N., and Naora, H. (2014) P-cadherin promotes ovarian cancer dissemination through tumor cell aggregation and tumor-peritoneum interactions. *Mol. Cancer Res.* **12**, 504–513
13. Poland, J., Sinha, P., Siegert, A., Schönölzer, M., Korf, U., and Hauptmann, S. (2002) Comparison of protein expression profiles between monolayer and spheroid cell culture of HT-29 cells revealed fragmentation of CK18 in three-dimensional cell culture. *Electrophoresis* **23**, 1174–1184
14. Leung, F., Musrap, N., Diamandis, E. P., and Kulasingam, V. (2013) Advances in mass spectrometry-based technologies to direct personalized medicine in ovarian cancer. *Transl. Proteom.* **1**, 74–86
15. Ong, S. E., Blagojev, B., Kratchmarova, I., Kristensen, D. B., Steen, H., Pandey, A., and Mann, M. (2002) Stable isotope labeling by amino acids in cell culture, SILAC, as a simple and accurate approach to expression proteomics. *Mol. Cell. Proteomics* **1**, 376–386
16. Bendall, S. C., Hughes, C., Stewart, M. H., Doble, B., Bhatia, M., and Lajoie, G. A. (2008) Prevention of amino acid conversion in SILAC experiments with embryonic stem cells. *Mol. Cell. Proteomics* **7**, 1587–1597
17. Zietarska, M., Maugard, C. M., Filali-Mouhim, A., Alam-Fahmy, M., Tonin, P. N., Provencher, D. M., and Mes-Masson, A. M. (2007) Molecular description of a 3D *in vitro* model for the study of epithelial ovarian cancer (EOC). *Mol. Carcinog.* **46**, 872–885
18. Keller, G. M. (1995) *In vitro* differentiation of embryonic stem cells. *Curr. Opin. Cell Biol.* **7**, 862–869
19. Benjamini, H., and Hochberg, Y. (1995) Controlling the false discovery rate: a practical and powerful approach to multiple testing. *J. R. Stat. Soc. Ser. B Stat. Methodol.* **57**, 289–300
20. Livak, K. J., and Schmittgen, T. D. (2001) Analysis of relative gene expression data using real-time quantitative PCR and the 2 $(-\Delta\Delta C_T)$ method. *Methods* **25**, 402–408
21. Hegab, A. E., Sakamoto, T., Nomura, A., Ishii, Y., Morishima, Y., Iizuka, T., Kiwamoto, T., Matsuno, Y., Homma, S., and Sekizawa, K. (2007) Niflumic acid and AG-1478 reduce cigarette smoke-induced mucin synthesis: the role of hCLCA1. *Chest* **131**, 1149–1156
22. Zhou, Y., Shapiro, M., Dong, Q., Louahed, J., Weiss, C., Wan, S., Chen, Q., Dragwa, C., Savio, D., Huang, M., Fuller, C., Tomer, Y., Nicolaides, N. C., McLane, M., and Levitt, R. C. (2002) A calcium-activated chloride channel blocker inhibits goblet cell metaplasia and mucus overproduction. *Novartis Found. Symp.* **248**, 150–165; discussion 165–170; 277–282
23. Francia, G., Man, S., Teicher, B., Grasso, L., and Kerbel, R. S. (2004) Gene expression analysis of tumor spheroids reveals a role for suppressed DNA mismatch repair in multicellular resistance to alkylating agents. *Mol. Cell. Biol.* **24**, 6837–6849
24. Puiffe, M. L., Le Page, C., Filali-Mouhim, A., Zietarska, M., Ouellet, V., Tonin, P. N., Chevrette, M., Provencher, D. M., and Mes-Masson, A. M. (2007) Characterization of ovarian cancer ascites on cell invasion, proliferation, spheroid formation, and gene expression in an *in vitro* model of epithelial ovarian cancer. *Neoplasia* **9**, 820–829
25. Sodek, K. L., Ringuette, M. J., and Brown, T. J. (2009) Compact spheroid formation by ovarian cancer cells is associated with contractile behavior and an invasive phenotype. *Int. J. Cancer* **124**, 2060–2070
26. Elschenbroich, S., Ignatchenko, V., Clarke, B., Kalloger, S. E., Boutros, P. C., Gramolini, A. O., Shaw, P., Jurisica, I., and Kislinger, T. (2011) In-

- depth proteomics of ovarian cancer ascites: combining shotgun proteomics and selected reaction monitoring mass spectrometry. *J. Proteome Res.* **10**, 2286–2299
27. Shender, V. O., Pavlyukov, M. S., Ziganshin, R. H., Arapidi, G. P., Kovalchuk, S. I., Anikanov, N. A., Altukhov, I. A., Alexeev, D. G., Butenko, I. O., Shavarda, A. L., Khomyakova, E. B., Evtushenko, E., Ashrafyan, L. A., Antonova, I. B., Kuznetsov, I. N., Gorbachev, A. Y., Shakhparonov, M. I., and Govorun, V. M. (2014) Proteome-metabolome profiling of ovarian cancer ascites reveals novel components involved in intercellular communication. *Mol. Cell. Proteomics* **13**, 3558–3571
 28. Gortzak-Uzan, L., Ignatchenko, A., Evangelou, A. I., Agochiya, M., Brown, K. A., St Onge, P., Kireeva, I., Schmitt-Ulms, G., Brown, T. J., Murphy, J., Rosen, B., Shaw, P., Jurisica, I., and Kislinger, T. (2008) A proteome resource of ovarian cancer ascites: integrated proteomic and bioinformatic analyses to identify putative biomarkers. *J. Proteome Res.* **7**, 339–351
 29. Faça, V. M., Ventura, A. P., Fitzgibbon, M. P., Pereira-Faça, S. R., Pitteri, S. J., Green, A. E., Ireton, R. C., Zhang, Q., Wang, H., O'Brian, K. C., Drescher, C. W., Schummer, M., McIntosh, M. W., Knudsen, B. S., and Hanash, S. M. (2008) Proteomic analysis of ovarian cancer cells reveals dynamic processes of protein secretion and shedding of extra-cellular domains. *PLoS One* **3**, e2425
 30. Gruber, A. D., Elble, R. C., Ji, H. L., Schreur, K. D., Fuller, C. M., and Pauli, B. U. (1998) Genomic cloning, molecular characterization, and functional analysis of human CLCA1, the first human member of the family of Ca²⁺-activated Cl⁻ channel proteins. *Genomics* **54**, 200–214
 31. Loewen, M. E., and Forsyth, G. W. (2005) Structure and function of CLCA proteins. *Physiol. Rev.* **85**, 1061–1092
 32. Frede, J., Fraser, S. P., Oskay-Özcelik, G., Hong, Y., Ioana Braicu, E., Sehouli, J., Gabra, H., and Djamgoz, M. B. (2013) Ovarian cancer: ion channel and aquaporin expression as novel targets of clinical potential. *Eur. J. Cancer* **49**, 2331–2344
 33. Li, M., Wang, Q., Lin, W., and Wang, B. (2009) Regulation of ovarian cancer cell adhesion and invasion by chloride channels. *Int. J. Gynecol. Cancer* **19**, 526–530
 34. Yang, B., Cao, L., Liu, B., McCaig, C. D., and Pu, J. (2013) The transition from proliferation to differentiation in colorectal cancer is regulated by the calcium activated chloride channel A1. *PLoS One* **8**, e60861
 35. Patel, A. C., Brett, T. J., and Holtzman, M. J. (2009) The role of CLCA proteins in inflammatory airway disease. *Annu. Rev. Physiol.* **71**, 425–449
 36. Hauber, H. P., Daigneault, P., Frenkiel, S., Lavigne, F., Hung, H. L., Levitt, R. C., and Hamid, Q. (2005) Niflumic acid and MSI-2216 reduce TNF- α -induced mucin expression in human airway mucosa. *J. Allergy Clin. Immunol.* **115**, 266–271
 37. Musrap, N., Karagiannis, G. S., Saraon, P., Batruch, I., Smith, C., and Diamandis, E. P. (2014) Proteomic analysis of cancer and mesothelial cells reveals an increase in Mucin 5AC during ovarian cancer and peritoneal interaction. *J. Proteomics* **103**, 204–215

Comparative Proteomics of Ovarian Cancer Aggregate Formation Reveals an Increased Expression of Calcium-activated Chloride Channel Regulator 1 (CLCA1)

Natasha Musrap, Alessandra Tuccitto, George S. Karagiannis, Punit Saraon, Ihor Batruch and Eleftherios P. Diamandis

J. Biol. Chem. 2015, 290:17218-17227.

doi: 10.1074/jbc.M115.639773 originally published online May 24, 2015

Access the most updated version of this article at doi: [10.1074/jbc.M115.639773](https://doi.org/10.1074/jbc.M115.639773)

Alerts:

- [When this article is cited](#)
- [When a correction for this article is posted](#)

[Click here](#) to choose from all of JBC's e-mail alerts

Supplemental material:

<http://www.jbc.org/content/suppl/2015/05/24/M115.639773.DC1.html>

This article cites 37 references, 7 of which can be accessed free at <http://www.jbc.org/content/290/28/17218.full.html#ref-list-1>